MHD FLOW OF A THIRD GRADE FLUID IN A CYLINDRICAL PIPE IN THE PRESENCE OF REYNOLDS' MODEL VISCOSITYAND JOULE HEATING

Supported by tetfund TERTIARY EDUCATION TRUST FUND

M. O. Iyoko[1]*, G. T. Okedayo[2], T. Aboiyar[1], and L. N. Ikpakyegh[1]

[1]Department of Mathematics/Statistics/Computer Science, University of Agriculture Makurdi, Benue State, Nigeria

[2]Department of Mathematics, Ondo State University of Science and Technology Okitipupa, Nigeria

*Corresponding author: mikiyoks@gmail.com, lewisnyitor@yahoo.com

Received: January 13, 2017 **Accepted:** March 18, 2017

Abstract: We investigated the flow of a third grade fluid through a cylindrical pipe in the presence of a magnetic field and joule heating, with the aim of finding approximate analytic solutions to the dimensionless velocity and temperature of the fluid. The Adomian decomposition method was applied to the dimensionless momentum and energy equations for the Reynolds' viscosity model case. In the absence of magnetic effect and joule heating we found a difference of at most 10^{-1} between the adomian decomposition solution and the perturbation solution of Jayeoba and Okoya. Graphs depicting the velocity and temperature distributions for various values of the thermo-physical parameters were plotted and analyzed, and it is observed that the magnetic field parameter decreases the velocity of the fluid and increases the temperature while the joule heating parameter reverses the effect of the heat generation parameter.

Keywords: Third grade fluid, Joule heating, Magnetohydrodynamics, adomian decomposition method

Introduction

Non-Newtonian fluids are fluids that do not obey the Newtonian constitutive equation; such fluids include polymers, paints, slurries, blood, lubricants, mud, pasta, personal care products, ice cream, oils, cheese, asphalt and many others. Most biological fluids with higher molecular weight components are also non-Newtonian in nature. They exhibit effects such as climbing of a rotating rod in an otherwise still container of fluid, self-siphoning, drag reduction, and transformation into a semisolid when an electric or magnetic field is applied.

The non-Newtonian fluids in particular have key importance in geophysics, chemical and nuclear industries, material processing, oil reservoir engineering, bioengineering and many others. Rheological properties of all non-Newtonian fluids cannot be predicted using simple constitutive equation (unlike the case of viscous fluids). Therefore many models of non-Newtonian fluids are based either on "natural" modifications of established macroscopic theories or molecular considerations. The additional rheological parameters in the constitutive equations of non-Newtonian fluids are the main culprit for the lack of analytical solutions. The resulting equations are more complex and of higher order than the Navier-Stokes equations. Hence these equations have been attractive from a modelling as well as solutions point of view (Hayat *et al.*, 2014).

For problems involving heat transfer, the third grade is of most interest to researchers in recent times due to its varied applications in science, industry and technology. Heat transfer problem of third-grade fluids without heat source term has been studied by several authors. Joule heating, also known as ohmic heating and resistive heating is the process by which the passage of an electric current through a conductor releases heat. The amount of heat released by the conductor is proportional to the square of the current passed through it. Since the work of James Prescott joule in 1841 and subsequently by Heinrich Lenz in 1842, several works on Joule heating has appeared in Literature; for example Aiyesimi *et al.* (2012) considered the combine effects of slip boundary, Ohmic heating on MHD flow of a third grade fluid down an inclined plane.

Magnetohydrodynamics (MHD) is the study of the interaction of electrically conducting fluids and electromagnetic forces (Raftari *et al.*, 2013). MHD problems arise in a wide variety of situations ranging from the explanation of the origin of the earth magnetic field and the prediction of space weather to the damping of turbulent fluctuations in semiconductor melts during crystal growth and even the measurement of the flow rates of beverages in the food industry (Smith, 1971; Branover and Gershon, 1976; Holroyd, 1979; Holroyd, 1980). Hartmann (1937) studied the influence of a transverse uniform magnetic field on the flow of viscous incompressible electrically conducting fluid between two finite parallel stationary and insulating plates.

Gbadeyan *et al.* (2014) used the method of regular and homotopy perturbations in their work on the effect of suction on thin film flow of a third grade fluid in a porous medium down an inclined plane in the presence of heat transfer. Costa and Sandberg (2004) developed a mathematical model to estimate burn rate, temperature profiles and positions of a natural smoldering log, while Makinde (2009) employed a novel hybrid numerical-analytical scheme based on a special type of Hermite-Pade approximants to examine the flow of a variable viscosity optically thin fluid through a channel with isothermal walls.

Jayeoba and Okoya (2012) studied a one-dimensional heat generation and viscous dissipation model of a third grade fluid in a cylinder. Their study considered both Reynolds' and Vogel's model viscosities, and the analysis was based on the regular perturbation technique. The heat transfer model was also solved numerically and the numerical solutions for special cases were found to agree excellently with previous ones obtained by the finite difference method.

The Adomian Decomposition Method (ADM) as a mathematical method was developed by George Adomian in the mid-eighties. The method is applied for solving both linear and nonlinear differential and integral equations. Siddiqui *et al.* (2010) used the Adomian decomposition method in the study of parallel plate flow of a third grade fluid where the results revealed the effectiveness and convenience of the Adomian decomposition method.

In this paper, we will extend the same model of Jayeoba and Okoya (2012). This extension involves including a magnetic effect term in the momentum equation and also a joule heating term in the energy equation of the existing model. The flow problem therefore becomes a Magnetohydrodynamic (MHD) flow problem. We shall consider the Reynolds' model viscosity, and use the Adomian Decomposition Method (ADM) to obtain approximate analytic solutions to the velocity and the temperature.

Description of the Model

An infinitely long cylinder is considered with the steady incompressible flow of a third grade fluid as can be seen in Fig. 1.

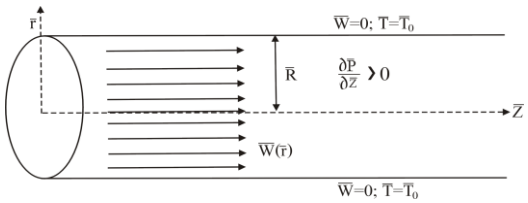

Fig. 1: Physical model and coordinate system

The equations for the velocity and the temperature, given by Massoudi and Christe (1995) as well as Yurusoy and Pakdemirli (2002), may be extended to incorporate a source term (Olajuwon, 2009) and further extended to incorporate a magnetic effect term and a joule heating term, and given by

$$\frac{1}{\bar{r}}\frac{d}{d\bar{r}}\left(\bar{r}(2\alpha_1+\alpha_2)\left[\frac{d\bar{\omega}}{d\bar{r}}\right]^2\right)=\frac{\partial\bar{p}}{\partial\bar{r}} \quad (1)$$

$$0=\frac{\partial\bar{p}}{\partial\phi} \quad (2)$$

$$\frac{1}{\bar{r}}\frac{d}{d\bar{r}}\left(\bar{r}\bar{\mu}\frac{d\bar{\omega}}{d\bar{r}}\right)+\frac{1}{\bar{r}}\frac{d}{d\bar{r}}\left(2\bar{r}\beta_3\left[\frac{d\bar{\omega}}{d\bar{r}}\right]^3\right)-\sigma{\beta_0}^2\bar{\omega}=\frac{\partial\bar{p}}{\partial\bar{z}} \quad (3)$$

$$K\left(\frac{1}{\bar{r}}\frac{d}{d\bar{r}}\left(\bar{r}\frac{d\bar{T}}{d\bar{r}}\right)\right)+\bar{\mu}\left(\frac{d\bar{\omega}}{d\bar{r}}\right)^2+2\beta_3\left(\frac{d\bar{\omega}}{d\bar{r}}\right)^4+\overline{QC_0}(\bar{T}-\overline{T_0})+\sigma{\beta_0}^2\bar{\omega}^2=0 \quad (4)$$

The required boundary conditions to solve equations (3) and (4) are

$$\bar{\omega}(\bar{R})=\bar{T}(\bar{R})=0\ ,\ \frac{d\bar{\omega}}{d\bar{r}}(0)=\frac{d\bar{T}}{d\bar{r}}(0)=0 \quad (5)$$

where all symbols are defined in the Nomenclature. The source term $\bar{Q}$ represents the heat generation when $\bar{Q}>0$ and the heat absorption term when $\bar{Q}<0$. The term $\sigma{\beta_0}^2\bar{\omega}$ is the magnetic effect term while the term $\sigma{\beta_0}^2\bar{\omega}^2$ is the joule heating term. Here equation (3) is to be integrated for a given $\frac{\partial\bar{p}}{\partial\bar{z}}$ and once the flow field is determined, the actual pressure field can be obtained from equation (1) and (3). Equation (3) is called the momentum equation while equation (4) is called the energy equation.

The corresponding dimensionless equations for equations (3)-(5) are given as the following:

$$\frac{d\mu}{dr}\frac{d\omega}{dr}+\frac{\mu}{r}\left(\frac{d\omega}{dr}+r\frac{d^2\omega}{dr^2}\right)+\frac{\Lambda}{r}\left[\frac{d\omega}{dr}\right]^2\left(\frac{d\omega}{dr}+3r\frac{d^2\omega}{dr^2}\right)-H\omega=C \quad (6)$$

$$\frac{d^2\theta}{dr^2}+\frac{1}{r}\frac{d\theta}{dr}+\Gamma\left(\frac{d\omega}{dr}\right)^2\left(\mu+\Lambda\left(\frac{d\omega}{dr}\right)^2\right)+\delta\theta+J\omega^2=0 \quad (7)$$

With boundary conditions

$$\omega(1)=\theta(1)=0,\frac{d\omega}{dr}(0)=\frac{d\theta}{dr}(0)=0 \quad (8)$$

The form of equations (6) and (7) depends on the viscosity model, and the viscosity μ is assumed to be a function of temperature. We now present the Reynold's model case as can be found in Massoudi and Christe (1995), Pakdemirli and Yilmas (2006), Nadeem and Ali (2009), and Okoya (2011).

Here,

$$\bar{\mu}(\bar{T})=\bar{\mu}_0 exp(-\bar{M}(\bar{T}-\overline{T_0})) \quad (9)$$

It is well known that Reynolds viscosity decreases with increasing temperature for liquids whenever M is positive, and it increases with increasing temperature for gas whenever M is negative. When M is large, then the effect of variable viscosity can be neglected. The corresponding non-dimensional form of equation (9) is

$$\mu=exp(-\rho\theta). \quad (10)$$

The coupled nonlinear ordinary differential equations (6) and (7), with the boundary conditions (8), can be solved in principle by several methods, the Adomian decomposition method being a convenient and effective tool. Here, we shall use the Adomian decomposition method to determine the flow field and thermal distribution.

Analytical solutions

In this section, the Adomian decomposition method series solution will be obtained for the dimensionless velocity and temperature by using the Reynolds' model viscosity.

Taking the Maclaurin's series expansion of the exponential term, we can express equation (10) as

$$\mu=1-\rho\theta+O(\rho^2) \quad (11)$$

This implies that

$$\mu^{-1}=1+\rho\theta+O(\rho^2) \quad (12)$$

We can write equation (6) as

$$\frac{d^2\omega}{dr^2}+\frac{1}{r}\frac{d\omega}{dr}+\mu^{-1}\frac{d\mu}{dr}\frac{d\omega}{dr}+\frac{\Lambda}{r}\mu^{-1}\left[\frac{d\omega}{dr}\right]^3+3\Lambda\mu^{-1}\left[\frac{d\omega}{dr}\right]^2\frac{d^2\omega}{dr^2}-\mu^{-1}H\omega=C\mu^{-1} \quad (13)$$

With the operator L = $\frac{d^2}{dr^2}$ and R = $\frac{d}{dr}$, applying the inverse operator$L^{-1}=\iint(\cdot)drdr$ to both sides of equation (13) and (7) we have equation (14) and (15) respectively

$$\omega(r)=A+Br+CL^{-1}\mu^{-1}-L^{-1}\frac{1}{r}R\omega-L^{-1}(\mu^{-1}R\mu R\omega)-\Lambda L^{-1}\left(\frac{1}{r}\mu^{-1}[R\omega]^3\right)-3\Lambda L^{-1}(\mu^{-1}[R\omega]^2L\omega)+HL^{-1}(\mu^{-1}\omega) \quad (14)$$

$$\theta(r)=C+Dr-\delta L^{-1}\theta-JL^{-1}\omega^2-L^{-1}\frac{1}{r}R\theta-\Gamma L^{-1}(R\omega)^2(\mu+\Lambda(R\omega)^2) \quad (15)$$

Assuming solutions of the form

$$\omega(r)=\sum_{n=0}^{\infty}\omega_n \quad (16)$$

$$\theta(r)=\sum_{m=0}^{\infty}\theta_m \quad (17)$$

Substituting the series solutions (16) - (17) into equations (11) - (15) and making a one-to-one correspondence between the contributions on the LHS and the terms on the RHS,

For various values of the pressure gradient parameter C when the value of the other parameters are kept at unity we obtain the following three point approximations for the velocity and temperature profile as

$$\omega_{C=-0.75}(r)=-0.01772002738r^{10}+0.02025560957+9.887908975\times10^{-9}r^{20}-0.4479661466r^6+0.1499526588r^8+0.6712571033r^4+0.00001349679802r^{16}-0.3750000000r^2-0.00007954884039r^{14}-0.0007167841124r^{12}+0.000003628620709r^{18} \quad (18)$$

$$\omega_{C=-0.5}(r)=3.633631605\times10^{-9}r^{18}-0.009846098606r^6+0.07275928523r^4-0.2500000000r^2-1.931872170\times10^{-7}r^{16}+0.0007386087464r^8+0.1862191412+0.0001761828104r^{10}-0.00005323154209r^{12}+3.440878554\times10^{-10}r^{20}+0.000006301214574 \quad (19)$$

$$\omega_{C=-1}(r)=-2.235471393r^{10}+0.9570273808-0.002203048840r^{16}-2.146740237r^6+0.0003457153478r^{18}+2.890769849r^8-0.03227424855r^{12}+0.9756509760r^4+1.201568584\times10^{-7}r^{20}+0.09289488443r^{14}-\frac{1}{2}r^2 \quad (20)$$

$$\theta_{C=-0.75}(r)=0.1256928962-0.03977055348r^{10}+0.1329355178r^8-0.2156315259r^6-0.008545021160r^4+0.005651780245r^{12}-0.0003321070340r^{14}-9.869264018\times10^{-7}r^{16} \quad (21)$$

$$\theta_{C=-0.5}(r) = 0.04114004201 + 0.00001308243597r^{12} - 0.0003301319317r^{10} + 0.002753269621r^{8} - 0.01575258075r^{6} - 1.361325848 \times 10^{-8}r^{16} - 0.02782356590r^{4} - 1.018625134 \times 10^{-7}r^{14} \quad (22)$$

$$\theta_{C=-1}(r) = 0.6230815902 + 0.2127691609r^{12} - 0.195290827r^{6} - 0.2864074205r^{10} + 0.164578053r^{8} - 0.4482126262r^{4} - 0.07051288447r^{14} - 0.00002593824319r^{16} \quad (23)$$

Computational result showing the difference between adomian decomposition and perturbation solutions

For the purpose of comparison, the mid plane temperature distribution of the pipe $\theta(0) = \theta_{max}$ for the obtained Adomian decomposition method solution (ADM) when $H = J = 0$, and the perturbation solution (P) of Jayeoba and Okoya (2012) are tabulated. The difference between the solutions obtained by the two methods is also computed.

Table 1: Difference between the value of $\theta_{max}(ADM)$ and $\theta_{max}(P)$ when $\Gamma = \delta = \rho = 1$

$\lvert C\rvert$		$\Lambda = 1$	
	$\theta_{max}(ADM)$	$\theta_{max}(P)$	Difference
0.25	0.01057	0.00187	8.70×10^{-3}
0.5	0.04400	0.00485	3.92×10^{-2}
0.75	0.10500	0.01025	9.48×10^{-2}
1	0.20000	0.01754	1.82×10^{-1}
2	1.04000	0.05154	9.88×10^{-1}
Λ		$C = -1$	
	$\theta_{max}(ADM)$	$\theta_{max}(P)$	Difference
0	0.14286	0.01928	1.24×10^{-1}
0.5	0.17143	0.01841	1.53×10^{-1}
1	0.20000	0.01754	1.82×10^{-1}
1.1	0.20571	0.01737	1.88×10^{-1}
1.5	0.22857	0.01668	2.12×10^{-1}

Table 2: Difference between the value of $\theta_{max}(ADM)$ and $\theta_{max}(P)$ when $\Lambda = -C = \rho = 1$

Γ		$\delta = 1$	
	$\theta_{max}(ADM)$	$\theta_{max}(P)$	Difference
0	0.0	0.0	0.0
1	0.20000	0.01754	1.82×10^{-1}
3	0.46667	0.05373	4.13×10^{-1}
5	0.63636	0.09138	5.45×10^{-1}
6	0.70000	0.11076	5.89×10^{-1}
δ		$\Gamma = 1$	
	$\theta_{max}(ADM)$	$\theta_{max}(P)$	Difference
-0.4	0.09091	0.01268	7.82×10^{-2}
-0.2	0.09859	0.01338	8.52×10^{-2}
0	0.10769	0.01407	9.36×10^{-2}
0.5	0.14000	0.01581	1.24×10^{-1}
1	0.20000	0.01754	1.82×10^{-1}

Table 3: Difference between the value of $\theta_{max}(ADM)$ and $\theta_{max}(P)$when$\Gamma = \Lambda = -C = 1$

ρ		$\delta = 1$	
	$\theta_{max}(ADM)$	$\theta_{max}(P)$	Difference
-6	$-$	0.01626	$-$
-4	0.70000	0.01663	6.83×10^{-1}
0	0.23333	0.01736	2.16×10^{-1}
5	0.12727	0.01828	1.09×10^{-1}
6	0.11666	0.01846	9.82×10^{-2}

In Table 1, we see that for $|C| \leq 0.75$ the Adomian decomposition and perturbation solutions agree in a very good way with the difference less than 10^{-1} when $\Gamma = \delta = \rho = \Lambda = 1$. We considered the variation of the non-Newtonian parameter (Λ) in Table 1, column 5 - 8. For all the values of Λ the difference is 10^{-1}. In Table 2, column 1 - 4, Γ is varied and the difference between the two solutions is observed to be at most 10^{-1} for all its values. The variation of the heat generation/absorption parameter δ is investigated in column 5-8 of Table 2. The adomian decomposition and perturbation solutions have a very good agreement with the difference less than 10^{-1} for $-0.4 \leq \delta \leq 0$. In Table 3, the difference between the two solutions is 10^{-1} for all the values of ρ.

Results and Discussion

The analytical solutions (18) – (23) for the dimensionless velocity and temperature distributions, as well as those for the other thermo-physical parameters are plotted against the radius of the pipe. The velocity profiles for the different thermo-physical parameters are represented by Figs. 2 – 8 while the temperature profiles are represented by Figs. 9 – 15. In these figures, the variations of the thermo-physical parameters are taken into account.

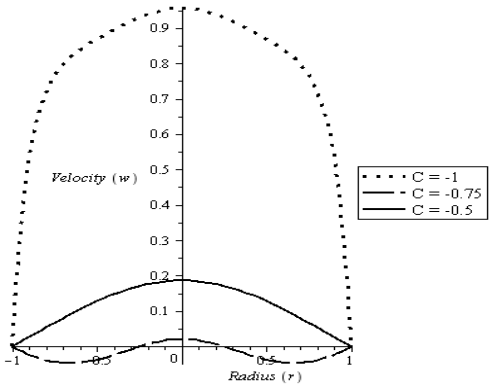

Fig. 2: Velocity profiles for various values of the pressure gradient parameter C with $H = \Gamma = J = \delta = \Lambda = \rho = 1$

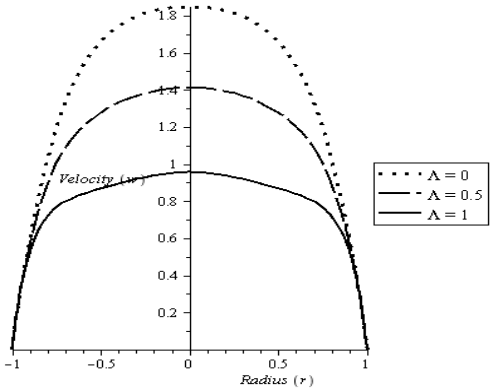

Fig. 3: Velocity profiles for various values of the non-newtonian material parameter of the fluid Λ with $H = \Gamma = J = \delta = -C = \rho = 1$

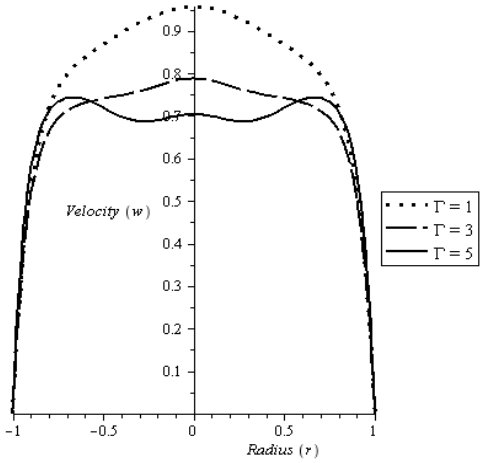

Fig. 4: Velocity profiles for various values of the viscous dissipation parameter Γ with $H = J = \delta = -C = \Lambda = \rho = 1$

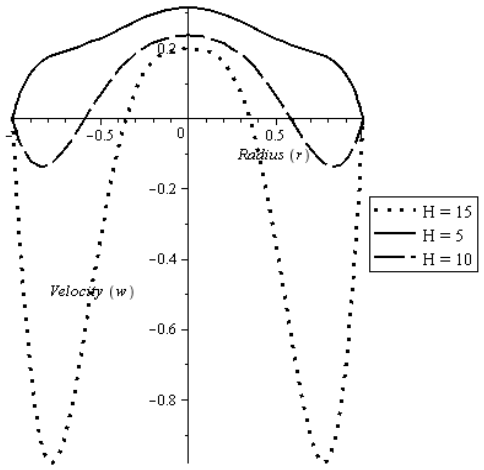

Fig. 5: Velocity profiles for various values of the magnetic effect parameter H with $\Gamma = J = \delta = -C = \Lambda = \rho = 1$

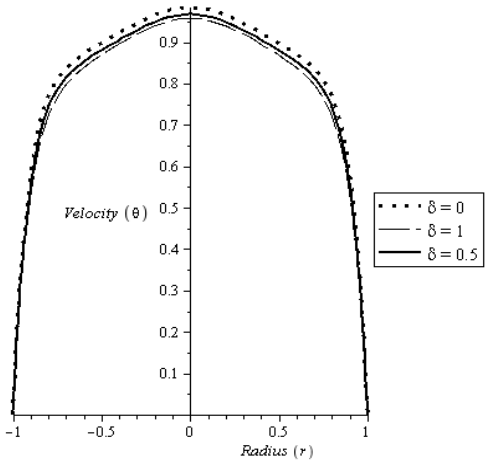

Fig. 6: Velocity profiles for various values of the heat generation parameter δ with $H = \Gamma = J = -C = \Lambda = \rho = 1$

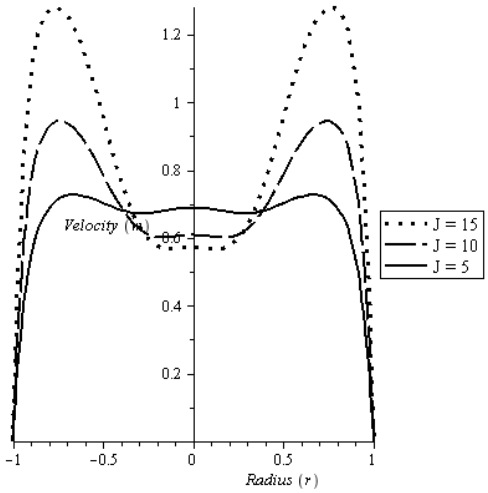

Fig. 7: Velocity profiles for various values of the Joule heating parameter J with $H = \Gamma = \delta = -C = \Lambda = \rho = 1$

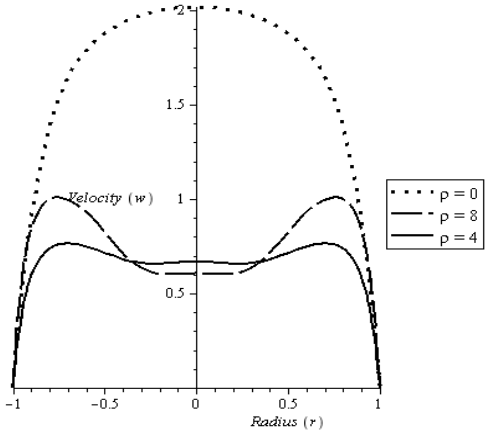

Fig. 8: Velocity profiles for various values of the Reynolds' viscosity variational parameter ρ with $H = \Gamma = J = \delta = -C = \Lambda = 1$

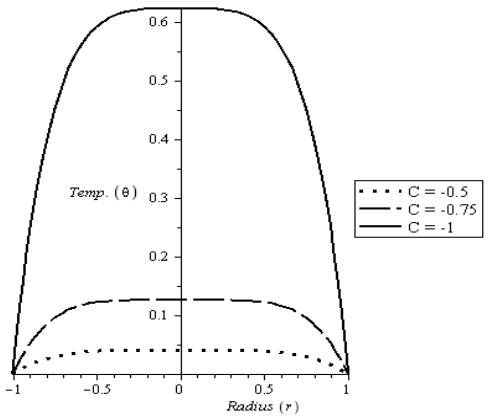

Fig. 9: Temperature profiles for various values of the pressure gradient parameter C with $H = \Gamma = J = \delta = \Lambda = \rho = 1$

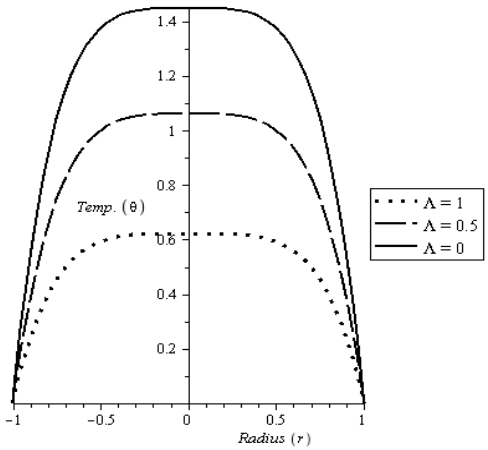

Fig. 10: Temperature profiles for various values of the non-newtonian material parameter of the fluid Λ with $H = \Gamma = J = \delta = -C = \rho = 1$

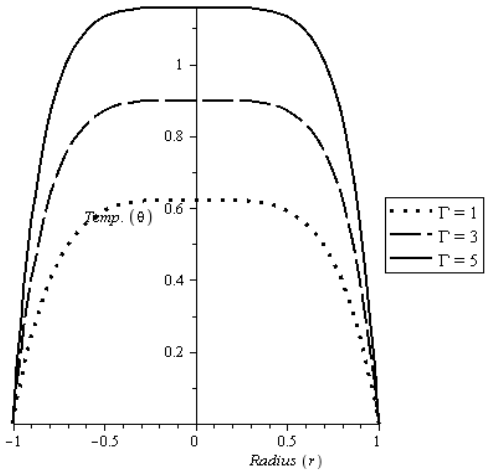

Fig. 11: Temperature profiles for various values of the viscous heating parameter Γ with $H = J = \delta = -C = \Lambda = \rho = 1$

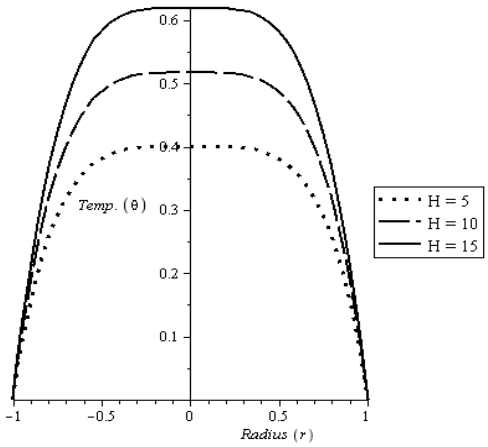

Fig. 12: Temperature profiles for various values of the magnetic effect parameter H with $\Gamma = J = \delta = -C = \Lambda = \rho = 1$

Figures 2 and 9 are the velocity and temperature profiles for various values of the pressure gradient parameter C, when the values of the other thermo-physical parameters are equal to one (1), respectively. In Fig. 2, the maximum velocity occurs at the point $r = 0$ which is the middle of the pipe. As the value of C drops from -0.5 to -0.75 the maximum velocity decreases, but further drop in the value of the pressure gradient parameter to -1 brings about an increment in the maximum velocity. Meanwhile, in Fig. 9 the maximum temperature of the fluid which also occurs at the middle of the pipe consistently increases as the value of the pressure gradient parameter C becomes more negative from -0.5 to -1.

Figures 3 and 10 reveal the effect of the non-Newtonian material parameter of the fluid Λ on the velocity and temperature profiles respectively. In Fig. 3, it is observed that as the value of Λ increases the maximum velocity at the middle of the pipe decreases. Increase in the value of Λ also results in a decrease in the maximum temperature of the fluid at the middle of the pipe, as can be seen in Fig. 10. The case when $\Lambda = 0$ corresponds to a Newtonian fluid.The velocity and temperature distribution for various values of the viscous dissipation parameter Γ is presented in Fig. 4 and 11 respectively. Increase in values of Γ tends to decrease the velocity of the fluid as can be observed in Fig. 4. Whereas, in Fig. 11 increase in the value of Γ appears to increase the temperature of the fluid due to the irreversible conversion of mechanical energy to thermal energy, which is in good agreement with Jayeoba and Okoya (2012).

The influence of various values of the magnetic effect parameter H on the dimensionless velocity and temperature is depicted by Fig. 5 and 12, respectively. In Fig. 5, increment in the value of H brings about a reduction in the velocity of the fluid; this is seen as the value of the velocity becomes negative. This agrees with the fact that non-Newtonian fluids become semi-solids in the presence of a magnetic field. From Fig. 12, it is evident that increase in the value of the magnetic effect parameter increases the temperature of the fluid, which is maximum at the middle of the pipe.

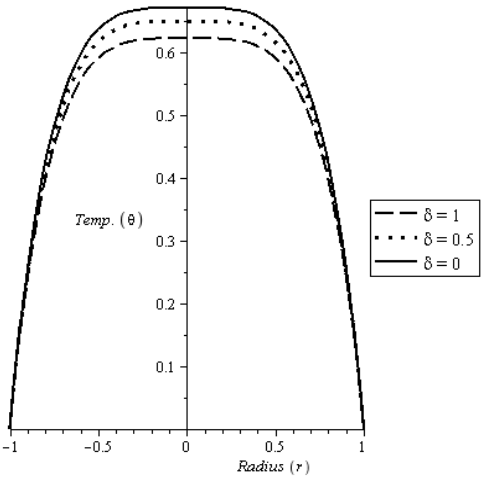

Fig. 13: Temperature profiles for various values of the heat generation parameter δ with $H = \Gamma = J = -C = \Lambda = \rho = 1$

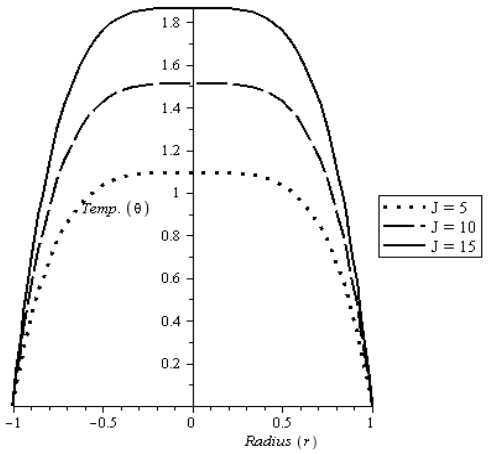

Fig. 14: Temperature profiles for various values of the Joule heating parameter J with $\mathrm{H} = \Gamma = \delta = -\mathrm{C} = \Lambda = \rho = 1$

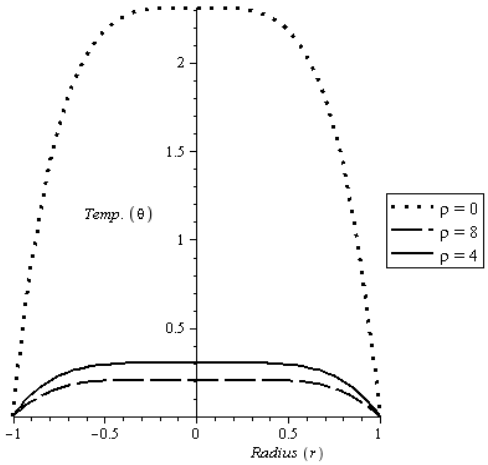

Fig. 15: Temperature profiles for various values of the Reynolds' viscosity variational parameter ρ with $\mathrm{H} = \Gamma = J = \delta = -\mathrm{C} = \Lambda = 1$

The effect of the heat generation parameter δ on the velocity and temperature is shown in Fig. 6 and 13, respectively. Fig. 6 indicates that as the value of δ increases the velocity falls. Fig.13 also indicates a decrease in the temperature of the fluid as the value of δ increases. This is the opposite of the case by Jayeoba and Okoya (2012) and previous studies because those studies did not include Joule heating. The presence of Joule heating over rides the effect of the heat generation parameter. Fig. 7 and 14 portray the effect of the joule heating parameter J on the velocity and temperature of the fluid respectively. Fig. 7 shows that the maximum velocity occurs close to the wall of the pipe and then falls a little below this value at the middle of the pipe. As the value of J increases the velocity increases close to the pipe's wall and then decreases at the middle of the pipe. In Fig. 14, increases in the value of the joule heating parameter increases the temperature of the fluid. When J is relatively large the fluid finally exceeds the least temperature distribution.

The effect of the Reynolds' viscosity variational parameter ρ on the velocity and the temperature is depicted by Fig. 8 and 15. Fig. 8 shows that the velocity at the middle of the pipe decreases as the value of ρ increases. Similarly in Fig. 15, increase in ρ results in a reduction in the temperature at the middle of the pipe. The case of constant viscosity corresponds to when $\rho = 0$.

Conclusions

In this paper we extended the model equations of Jayeoba and Okoya (2012) by incorporating a magnetic effect term in the momentum equation and a joule heating term in the energy equation. This extension gave rise to a magnetohydrodynamic flow problem of a third grade fluid through a cylindrical pipe, which was solve by the Adomian decomposition method. A three point approximate analytical solution to the momentum and energy equations were obtained using the computer software Mapple (13). The results for various values of the thermo-physical parameters were presented in graphs, from which we make the following conclusions:

i. The more negative the value of the pressure gradient parameter becomes, the higher the velocity and temperature of the fluid.
ii. Increase in the non-Newtonian material parameter of the fluid decreases the velocity and the temperature of the fluid.
iii. Increase in the viscous dissipation parameter decreases the velocity of the fluid and increases its temperature.
iv. The magnetic effect parameter reduces the velocity of the fluid and increases the temperature.
v. The effect of the heat generation parameter is reversed in the presence of joule heating.
vi. Increases in the Reynolds' viscosity parameter results in the decrease in both the velocity and temperature of the fluid.

Nomenclature

$\bar{r}$	Dimensional perpendicular dist. from pipe axis
$r = \bar{r}/\bar{R}$	Dimensionless perpendicular distance from pipe axis
$\bar{R}$	Radius of the pipe
$\bar{T}_0$	The initial temperature
$\bar{\omega}(\bar{R})$	Dimensional velocity component in the $\bar{z}$ axis
$\omega = \bar{\omega}/\bar{\omega}_0$	Dimensionless velocity component in the $\bar{z}$ axis
$\bar{\omega}_0$	Dimensional reference velocity
$\bar{z}$	Axis of the cylinder
$C = (\bar{R}^2/\bar{\omega}_0\bar{\mu}_0)(\partial\bar{p}/\partial\bar{z})$	Pressure gradient parameter
K	Constant thermal conductivity
$\partial\bar{p}/\partial\bar{r}$	Pressure gradient along the normal to the pipe axis
$\partial\bar{p}/\partial\bar{z}$	Pressure gradient in the axial direction
$\partial\bar{p}/\partial\phi$	Pressure gradient in rotational direction
$\bar{Q}$	Heat generation constant
$\overline{C_0}$	Initial concentration of the reactant species

Greek symbols	
α_1, α_2, and β_3	Constant material coefficients
$\beta = R\overline{T_0}/E$	Activation energy
$\rho = \overline{M}\beta\overline{T_0}$	Reynold's viscosity variational parameter
$\bar{\mu}$	Dynamic shear viscosity
$\mu = \bar{\mu}/{\bar{\mu}_0}^e$, ${\bar{\mu}_0}^e = \{\bar{\mu}_0 \; or \; \bar{\mu}_* = \bar{\mu}_0 \exp(\overline{T_0})\}$	Dimensionless viscosity
ϕ	Rotational direction
$\theta = (\bar{T} - \overline{T_0})E/\left(R{\overline{T_0}}^2\right)$	Dimensionless temperature excess
$\Gamma = \; 4{\bar{\mu}_0}^e{\bar{\omega}_0}^2/\kappa\beta\overline{T_0}$	Viscous heating parameter
$\Lambda = \beta_3{\bar{\omega}_0}^2/\bar{\mu}_0{\bar{r}_0}^2$	Non-Newtonian material parameter of the fluid
$\delta \; = \bar{Q}EA_0\bar{R}^2\overline{C_0}/KR{\overline{T_0}}^2$	Heat generation parameter
$H = \sigma\bar{R}^2{\beta_0}^2/\bar{\mu}_0$	Magnetic effect parameter
$J = \; E\bar{R}^2\sigma{\beta_0}^2{\bar{\omega}_0}^2/KR{\overline{T_0}}^2$	Joule heating parameter

References

Adomian GA 1992. A review of the decomposition method and some results for non-linear equation. *Maths. & Computer Modelling*, 13(7): 17-43.

Adomian GA 1994. Solving Frontier Problems of Physics: The Decomposition Method, Volume 60, Dordrecht, Kluwer Academic Publishers, p. 370.

Aiyesimi YM, Okedayo GT & Lawal OW2012a. MHD flow of a third grade fluid with heat transfer and slip boundary condition down an inclined plane. *Maths. Theory & Modeling*, 2(9): 108-120.

Aiyesimi YM, Abah SO & Okedayo GT 2012b. Radiative Effects on the Unsteady Double Diffusive MHD Boundary Layer Flow over a Stretching Vertical Plate. *Am. J. Scient. Res.*, 65: 51-61.

Alfvn H 1942. Existence of Electromagnetic-hydrodynamic Wave. *Nature*, 150: 405-406.

Branover H & Gershon P 1976. MHD Turbulence Study. Report BGUN-RDA-100-176. Ben-Gurion University.

De T, Costa S &Sandberg D 2004. Mathematical model of a smoldering log. *Combustion and Flame*, 139: 227-238.

Gbadeyan JA, Idowu AS, Okedayo GT, Ahmed LO & Lawal OW 2014. Effect of suction on thin film flow of a third grade fluid in a porous medium down an inclined plane with heat transfer. *Int. J. Scient. & Engr. Res.*, 5(4): 748-754.

Hartmann JI 1937. Hydrodynamics, theory of laminar flow of an electrically conducting liquid in a homogeneous magnetic field. *Int. Kongelige Danske Videnskabernes Selskab Matematisk-Fysiske Meddelelser*, 15: 1-27.

Hayat T, Shafiq A & Alsaedi A 2014. Effect of joule heating and thermal radiation in flow of third grade fluid over radiative surface. *Public Library of Sci. (PLoS One)*, 9(1): e83153.

Holroyd RJ 1979. An experimental study of the effect of wall conductivity, non-uniform magnetic field and variable-area ducts on liquid metal flow at high hartmann number, Part 1: Ducts with non-conducting wall. *J. Fluid Mechanics*, 93: 609-630.

Holroyd RJ 1980. MHD flow in a rectangular duct with pairs of conducting and non-conducting walls in the presence of a non-uniform magnetic field. *J. Fluid Mechanics*, 96: 335-3.

Jayeoba OJ & Okoya SS 2012. Approximate analytical solutions for pipe flow of a third grade fluid with variable models of viscosities and heat generation/absorption. *J. Nig. Maths. Soc.*, 31: 207-227.

Makinde OD 2009. Hermite- pade approach to thermal radiation effect on inherent irreversibility in a variable viscosity channel flow. *Computers & Maths. Applic.*, 58: 2330-2338.

Massoudi M & Christe I 1995. Effect of variable viscosity and viscous dissipation on the flow of third grade fluid in a pipe. *Int. J. Non-linear Mechanics*, 30(5): 687-699.

Okoya SS 2011. Disappearance of criticality for reactive third grade fluid with reynold's model viscosity in a flat channel. *Int. J. Non-linear Mechanics*, 46(9): 1110-11.

Olajuwon BI 2009. Flow and natural convection heat transfer in a power law fluid past a vertical plate with heat generation. *Int. J. Non-linear Sci.*, 7(1): 50-56.

Pakdemirli M & Yilbas BS 2006. Entropy generation for pipe flow of a third grade fluid with Vogel model viscosity. *Int. J. Non-linear Mechanics*, 41(3): 432-437.

Raftari B, Parvaneh F & Vajravelu K 2013. Homotopy analysis of the magnetohydrodynamic flow and heat transfer of a second grade fluid in a porous channel. *Energy*, 59: 625-632.

Siddiqui AM, Hameed M, Siddiqui BM &Ghori QK 2005. Use of adomoian decomposition method in the study of parrallel plate flow of a third grade fluid. *Int. J. Non-linear Mechanics*, 40: 807-820.

Smith P 1971. Some asymtoticextremum principle for magnetohydrodynamic pipe flow. *Appl. Sci. Resou.*, 24: 452-466.

Yurusoy M & Pakdemirli M 2002. Approximate analytical solution for the flow of a third grade fluid in a pipe. *Int. J. Non-linear Mechanics*, 37(2): 187-195.